



HAL
open science

EVOLUTION OF OXIDE SCALES ON FeAl GRADE 3 INTERMETALLIC ALLOY

Fernando Pedraza, Jean-Luc Grosseau-Poussard, J.F Dinhut

► **To cite this version:**

Fernando Pedraza, Jean-Luc Grosseau-Poussard, J.F Dinhut. EVOLUTION OF OXIDE SCALES ON FeAl GRADE 3 INTERMETALLIC ALLOY. *Intermetallics*, 2005, 13, pp.27-33. 10.1016/j.intermet.2004.04.042 . hal-00512816

HAL Id: hal-00512816

<https://hal.science/hal-00512816>

Submitted on 1 Sep 2010

HAL is a multi-disciplinary open access archive for the deposit and dissemination of scientific research documents, whether they are published or not. The documents may come from teaching and research institutions in France or abroad, or from public or private research centers.

L'archive ouverte pluridisciplinaire **HAL**, est destinée au dépôt et à la diffusion de documents scientifiques de niveau recherche, publiés ou non, émanant des établissements d'enseignement et de recherche français ou étrangers, des laboratoires publics ou privés.

EVOLUTION OF OXIDE SCALES ON FeAl GRADE 3 INTERMETALLIC ALLOY

F. Pedraza¹, J.L. Grosseau-Poussard², J.F. Dinhut^{2*}

LEMMA, Université de La Rochelle. 25, rue Enrico Fermi, 17042 La Rochelle cédex 1, FRANCE.

* Corresponding author: Phone: +33 (0)546458672, Fax: +33 (0)546457272, e-mail: fpedraza@univ-lr.fr

Abstract

The ODS FeAl Grade 3 intermetallic alloy have been shown to develop a structured oxide scale upon isothermal oxidation between 850 and 950° C for 24 h. Transmission electron microscopy studies have revealed a top nanoequiaxed alumina, central alumina and bottom Fe-Al spinel. At 1000° C, the spinel phase no longer forms but a columnar alumina layer topped up with a nanoequiaxed structure. The role of yttria is negligible at lower temperatures whereas some segregation at the scale/substrate interface and precipitation of YAlO₃ is observed at 1000° C.

Keywords: Iron aluminides (based on FeAl), oxidation.

1.- Introduction

The oxidation behaviour of Fe₃Al has been investigated by alloying it with chromium or titanium [1]; with and without zirconium [2], with and without yttrium [3] and with alumina and yttria dispersion [4]. In all these studies [1-3], the formation of the metastable and/or the protective phase of alumina has been reported depending on the oxidation temperature and time. Only Pint et al. [4] have indicated the formation of iron oxides developing at the surface at temperatures below 1000° C.

However, aluminides based on FeAl exhibit better oxidation and corrosion resistance than Fe₃Al alloys [5] as well as better sulphidation and carburisation resistance than the traditional heat resistant alloys [6]. Again, most of the studies conducted on either the binary FeAl or its yttrium oxide dispersion strengthened (ODS) counterpart have indicated the exclusive development of alumina phases [7-9], the yttria content affecting the extent of the metastable θ or the stable α phases [10]. However, in a more recent

study [11] the formation of an iron rich layer underneath that of alumina was observed to exist in binary FeAl. It can therefore be anticipated that this may oxidise by oxygen inward diffusion through the defects and the grain boundaries contained in the outer oxide scale. In this work, electron microscopy studies are carried out so as to ascertain the development of oxide scales at increasing temperatures in the ODS intermetallic alloy FeAl Grade 3.

2.- Experimental Procedure

The ODS intermetallic alloy was manufactured by CEA/CEREM (Grenoble, France) under the name of FeAl40 Grade 3, which contains 15 ppm B, 0.1 wt% Zr and a 1wt% Y₂O₃ dispersion. The material is mechanically alloyed and subsequently extruded at 1100° C. Therefore, it shows a strong <110> fibre texture and about 0.5-1 µm grain size [9,12]. Circular samples were cut from the rods to obtain discs of 15 mm diameter, 1 mm thick, which were subsequently mechanically polished to a final roughness of 0,01 µm. They were then ultrasonically degreased in acetone and rinsed in 96 % ethanol.

Isothermal oxidation runs were carried out in a Setaram TGA-92 thermobalance (10⁻⁶ g accurate) between 800 and 1000°C. A constant heating rate of 50°C.min⁻¹ was set under pure Ar gas before achieving the test temperatures. After 24 h of exposure, the samples were cooled at the rate of 50°C.min⁻¹ under the same flow of synthetic air (0.6 l.min⁻¹).

Characterisation of the oxidised specimens was undertaken by X-ray diffraction in a Bruker AXS D-5005 equipment in the θ -2 θ configuration using the Cu K α 1 (λ = 0.15406 nm) as well as by scanning electron microscopy (SEM) coupled to energy-dispersive spectrometry (EDS) in a JEOL JSM-4510 LV. Cross sections of the implanted specimens were also prepared for transmission electron microscopy (TEM) studies in a JEOL-JEM 2010 operating at 200 kV. Preparation of the TEM specimens involved cutting bars of 1x1x10 mm with a 1 µm diamond saw. Then the specimens were glued back to back using a conventional glue, while manually pressing for the removal of the excess of glue and let to dry out for at least 24 h. Following to it, the glued rectangular bars set into a brass cylinder, filled with epoxy resin and let to dry out for at least another 24 h. Finally, discs of 100 µm were sectioned using the 1 µm diamond saw, followed by careful mechanical polishing in SiC# 4000 emery paper

down to a thickness of about 50 μm . Then, Ar bombardment at 3.5 keV and 10-15 μA was carried out in a Gatan precision ion polishing system (PIPS™) model 691 alternating the ion beams with the two guns. The typical impinging angles were gradually decreased from 6 to 4.5°.

3.- Results

The oxidation kinetics of FeAl Grade 3 at the different tested temperatures have been presented in an earlier paper [11] showing a steady increase with temperature up to 1000° C, at which a slow down in oxygen intake was observed.

Fig. 1 shows the evolution of the oxide scale with increasing temperature. It can be observed that porosity decreases. No significant spallation takes place on any of the surfaces, but at 900 8C this phenomenon seems to be more prone to occur (Fig. 2). In this latter case, the scales seem to be composed by different species including isolated areas of $\theta\text{-Al}_2\text{O}_3$ with the typical plate-like morphology [10]. In the few spalled areas, voids of different size and shape are encountered, but further oxidation of the substrate is shown to occur by the outwardly growing light-coloured oxides.

Up to 950 °C SEM/EDS area analyses measured in plan-view on non-spalled oxide scales reveal constant Al/Fe atomic ratios of about 2 and at 1000 °C the Al content is almost five times greater than that of Fe. SEM/EDS microanalysis of the spalled and re-oxidised scales shows 1:1 contributions of Al and Fe. The X-ray diffractograms indicated the absence of the metastable θ -alumina phase at temperatures of 850 and 900 °C and a major peak at 950°C [11]. At 1000 °C only the stable α -alumina diffracted.

However, additional peaks had been recorded at 950 °C in the binary FeAl, which were claimed to possibly correspond to a spinel structure. According to the SEM cross-section studies, the oxide scales are generally well adhered and their thickness generally increase with oxidising temperature. At 1000 °C the scales are thinner and comparable to those developed at 850 °C (Table 1). However, TEM cross-section inspection at relatively high magnification of the scales grown at 850, 900 and 950 °C reveals a double structure as that shown in Fig. 3(a). The differences between them mainly arise from the total scale thickness. For instance, at 850 °C the scale is of about 0.3 μm

divided into an external layer of about 50 nm and an internal between 150 and 250 nm whereas at 950 μC , the total scale thickness is of about 1 μm . Between both layers, a flat interface develops, contrary to the wavy internal substrate/scale interface, which seems to result from internal oxidation of the substrate.

Table 1.- Oxidation rates and oxide thicknesses in ODS FeAl oxidised between 850 and 1000°C.

Temperature (°C)	k_p ($\text{mg}^2/\text{cm}^4\text{s})\times 10^{-7}$	Thickness (nm)	X-ray characterisation
850	0.8	170	B2 (+ $\alpha\text{-Al}_2\text{O}_3$)
950	2.7	650	B2 + $\theta\text{-Al}_2\text{O}_3$ (+ spinel)
1000	--	180	B2 + $\alpha\text{-Al}_2\text{O}_3$

The point TEM/EDS analyses performed with a 3 nm diameter spot through the scale thickness in cross-sectional studies indicate that the aluminium amount is constant whereas the amount of iron is higher at the bottom layer than at the scale/substrate interface. This may indicate constant outward flow of aluminium across such inner scale. At higher magnifications, a third top scale is found, which has an equiaxed morphology of nanometre scale [Fig. 3(b)]. A selected area diffraction patterns (SADP) of the overall scale is shown in Fig. 3(c) in which both the FeAl_2O_4 spinel and $\alpha\text{-Al}_2\text{O}_3$ oxides are present. At higher magnifications, it was found that the Fe/Al oxide was mainly located at the inner layer whereas alumina constituted the external one. The diffuse ring corresponding to a 2.07 Å d-spacing may indicate that the $\alpha\text{-Al}_2\text{O}_3$ at the gas/scale interface is nanosized. Table 2 summarises these results for further discussion. From a thermodynamic point of view, $\alpha\text{-Al}_2\text{O}_3$ is expected phase to develop in FeAl and a likely Al/Fe spinel layer on top depending on the experimental conditions. In Fe_3Al , iron rich oxides might be located above the alumina film [4]. In the present work, the formation and the location of the spinel phase can be considered as the result of a reaction between Al_2O_3 and Fe_2O_3 in such experimental conditions that the equilibrium has not been reached yet. However, it is to be noticed that the spinel oxide layer did not increase in thickness but the grains coarsened with increasing temperature.

Table 2.- Experimental d-spacings obtained from SADPs at the different oxide layers composing the scales developed in ODS FeAl oxidised between 850 and 950° C and their correspondence to the planes of the identified compounds.

d-spacing, Å	FeAl ₂ O ₄ (JCPDS 34-192)	α-Al ₂ O ₃ (JCPDS 83-2081)
4.65	111	-
2.84	220	-
2.46	311	-
2.05	400	113
1.67	422	-
1.55	511	-
1.44	440	-
1.16	444	-

At 1000 8C, the oxide scales show a completely different morphology. At this oxidising temperature, columnar grains of α-Al₂O₃ clearly develop from the substrate/scale interface as shown in Fig. 4(a). As marked between arrows in this image, the grains are topped with the previously shown equiaxed grains of nanometre scale seen clearly in Fig. 4(b). The overall thickness of the scale is as thin as about 200–250 nm. The TEM/EDS composition profiles across the oxide layer [Fig. 4(c)], show aluminium as the major metallic constituent. Yttrium seems to preferentially segregate at the oxide/substrate interface and all attempts to find this element at any other location of the oxide scale (including grain boundaries) were generally unsuccessful even in the dark field mode. However, some coarse grains of Y/Al oxide protruding into the alumina scale can be found occasionally as shown in Fig. 5. Besides, one of the grains shown in this image contains Zr embedded in it, as confirmed by TEM/EDS microanalysis.

4.- Discussion

The oxide scales covering more uniformly the substrate with increasing temperature is a natural phenomenon owing to the increase of diffusion enhancement of the species composing the oxide as long as side effects, such as spallation, remain negligible. In this work, spallation of the scale has rarely occurred and this has mostly been observed at 900 °C. The role of the yttrium oxide dispersion has often been reported to pin the grain boundaries of the alloy and to hinder dislocation movement within the grains [13] thus

enhancing the mechanical properties of the alloy [14–16]. However, the role of yttrium oxide concerning the scale adhesion to the iron-base intermetallics has been already investigated. However, most of the studies are devoted to NiAl and FeCrAl alloys, in which it has been found that yttrium diffuses outwardly and segregates at the alumina scale and at the gas/scale interface [17,18] enhancing adherence [19] by suppression of outward aluminium diffusion, which in turn seems to prevent void formation [20]. However, it has been revealed in Fig. 2 that when spallation occurs polygonal voids are encountered at the metal/scale interface, which seem to be associated with rapid outward aluminium diffusion. Czyska-Filemonowicz et al. [21,22] showed by microscopy techniques that an excessive amount of yttria could lead to a large number of cavities at the oxide grain boundaries as a result of microcrack formation at the grain boundaries of various (PM2000, PM2002 and MA956) ODS superalloys after oxidation at 1100 and 1200 °C for times of 5–1000 h. On the contrary, Montealegre et al. [9] observed spallation of the pure alumina scales without void formation at the scale/substrate interface after isothermal oxidation at 1100 °C of the same ODS FeAl (1 wt%Y₂O₃) of the present study, and explained such detachment in terms of the differences in the thermal expansion coefficients of the alumina and the metallic substrate upon cooling. However, they already claimed that a decrease in the yttria content would provide better results as those shown by Mignone et al. [7] in ODS FeAl with 0.5 wt% Y₂O₃.

The presence of significant amounts of iron at the internal part of the scales grown between 850 and 950 °C could indicate that the spinel oxide is very readily formed at the initial stages together with α -Al₂O₃ at the outermost surface [23]. This spinel oxide seems to originate from the reaction between Al₂O₃ and Fe₂O₃, as concluded from in situ high temperature XRD studies [24]. However, and according to the TEM/EDS analyses, aluminium diffusion seems to proceed faster during the following stages of oxidation giving rise to the development of the nanometre sized alumina thin scale on top of the FeAl₂O₄ layer. Equiaxed grained morphology has also been observed to occur in alumina scales developed on ODS FeCrAl alloys by countercurrent diffusion of oxygen and aluminium, with molecular oxygen transport occurring through defects developed in the scale [25]. In the present study, this may indicate that the inner FeAl₂O₄ layer may only be partially effective in hindering outward aluminium diffusion when the grains coarsen with increasing temperature [Fig. 4(a)] since aluminium is

typically transported by volume diffusion. Formation of θ - Al_2O_3 is nevertheless significantly impeded as this oxide has only been found on isolated areas of the surface, which is agreement with Montealegre and González-Carrasco [10], who in their studies at 900 and 1100 °C concluded that alumina formed from the earliest stages of oxidation on the 1% Y_2O_3 containing FeAl. Oxygen inward diffusion is not fully suppressed as indicated by the Al-rich oxide intrusions of the substrate material [Fig. 3(a)]. Although electron diffraction patterns are not available, α - Al_2O_3 might be the phase developing at the low oxygen partial pressure in these zones.

At 1000 °C, the top equiaxed thin layer again reflects the relatively high rates of nucleation and growth at the beginning of oxidation [26]. However, preferential inward oxygen diffusion seems to occur along the significant amount of grain boundaries oxidising the substrate so that columnar grains develop [20,25]. Ul-Hamid [27] showed by TEM that the alumina scales developed on Ni–10Cr–Al were not affected by the presence of yttrium in the early stages of oxidation, which agrees well with our observations. However, different Y–Al oxide phases have often been reported to stabilise the columnar structure of α - Al_2O_3 [21] by segregation of these phases at the alumina grain boundaries [22]. Gülgün et al. [28] described the mechanisms of yttrium segregation in α - Al_2O_3 between 1450 and 1650 °C and concluded that after adsorption and initial formation of yttrium aluminium garnet, equilibrium of this phase with alumina could occur, zirconium behaving in a similar manner. Since the solubility of yttrium in Al_2O_3 is below 1–2% [29], second phase particles thus precipitate [30]. In this study, the oxidation temperature never exceeded 1000 °C, temperature at which the more significant amount of yttria precipitates were found to segregate at the scale/alloy interface and coarsening of some grains also occurred (Fig. 5). Typically, the $\text{Y}_3\text{Al}_5\text{O}_{12}$ phases or $\text{Y}_4\text{Al}_2\text{O}_9$ are found to precipitate since they are stable whereas YAlO_3 is metastable [31]. However, calculations from the TEM/EDS microanalysis of the different areas of Fig. 5 would rather indicate that the grains are composed by YAlO_3 , with the embedded zirconium in the form of ZrO_2 . This provides an indication that in spite of their thermodynamic stability, the yttria dispersoids may coarsen and be transported outward [32]. However, the low density of these precipitates in the scale should not significantly influence the oxidation behaviour of the ODS FeAl, as concluded by Mennicke et al. [20].

5.- Summary

The ODS FeAl intermetallic alloy isothermally oxidised between 850 and 950 °C for 24 under synthetic air develops a three-layered structure in which a FeAl₂O₄ spinel phase composes the bottom layer, the centre and top layers being of alumina. At 1000 °C, only two layers are found to occur. The top alumina layer always shows an equiaxed structure arising from rapid inward and outward ion diffusion. Aluminium outward diffusion does not seem to be suppressed at these temperatures by the yttria dispersion nor by the inner Fe–Al spinel layer. However, metastable θ -Al₂O₃ oxide formation is significantly hindered. At 1000 °C, the spinel layer is no longer observable and a columnar alumina layer develops from the substrate towards the gas/scale interface. Yttria seems then to segregate at the scale/alloy interface and to randomly coarsen to produce an Y–Al oxide phase.

7.- Acknowledgements

This work was carried out under the post doctoral stay of F. Pedraza, funded by the Region of Poitou-Charentes (France).

6.- References

1. Babu N, Balasubramaniam R, Gosh A. *Corr. Sci.* 2001; 43: 2239.
2. Pint BA, Regina JR, Prussner K, Chitwood LD, Alexander KB, Tortorelli PF. *Intermetallics* 2001; 9:735.
3. Kim I, Cho WD, Kim HJ. *J. Mater. Sci.* 2000; 35:4695.
4. Pint BA, Leibowitz J, de Van JH., *Oxid. Met.* 1999; 51:181.
5. Deevi SC, Sikka VK. *Intermetallics* 1996; 4:357.
6. Tortorelli PF, Natesan K. *Mat. Sci. Eng.* 1998; A258:115.
7. Mignone A, Frangini S, La Barbera A, Tassa O. *Corr. Sci.* 1998; 40:1331.
8. Xu CH, Gao W, He YD., *Scripta Mater.* 2000; 42:975.
9. Montealegre MA, González-Carrasco JL, Morris-Muñoz MA, Chao J, Morris DG. *Intermetallics* 2000; 8:439.
10. Montealegre MA, González-Carrasco JL. *Intermetallics* 2003; 11:169.

11. Dang Ngoc Chan C, Huvier C, Dinhut JF. *Intermetallics* 2001; 9:817.
12. Dang Ngoc Chan C, Huvier C, Dinhut JF. *Surf. Coat. Technol.* 2003; 165:119.
13. Judkins RR, Rao US. *Intermetallics* 2000; 8:1347.
14. Tonneau A, Gerland M, Hénaff G. *Met. Mat. Trans.* 2001; 32A:2345.
15. Morris DG, García Oca C, Chao J, Muñoz-Morris MA. *Scripta Mater.* 2002; 46:843.
16. Muñoz-Morris MA, García Oca C, Morris DG, *Acta Mater.* 2002; 50:2825.
17. M.F. López, A. Gutiérrez, M.C. García-Alonso, M.L. Escudero, *J. Mater. Res.* 13 (12) (1998) 3411-3416.
18. Weinbruch S, Anastassiadis A, Ortner HM, Martinz HP, Wilhartitz P. *Oxid. Met.* 1999; 51:111.
19. García-Alonso MC, González-Carrasco JL, Pérez P, Haannappel VAC, Escudero ML, Chao J, Stroosnijder MF. *J. Mater.Sci. Mat. Med.* 2001; 12:589.
20. Mennicke C, Schumann E, Rühle M, Hussey RJ, Sproule GI, Graham MJ, *Oxid. Met.* 1998; 49:455.
21. Czyrska-Filemonowicz A, Clemens D, Quadackers WJ. *J. Mater. Proc. Technol.* 1995; 53:93.
22. Czyrska-Filemonowicz A, Szot K, Wasilkowska A, Gil A, Quadackers WJ, *Solid State Ionics* 1999; 117:13.
23. Pérez FJ, Pedraza F, Hierro MP, Balmain J, Bonnet G. *Oxid. Met.* 2002; 58:563.
24. Fujimura T, Tanaka SI. *J. Mater. Sci.* 1999; 34:425.
25. Quadackers WJ, Naumenko D, Singheiser L, Penkalla HJ, Tyagi AK, Czyrska-Filemonowicz A. *Mat. Corr.* 2000; 51:350.
26. Ul-Hamid A. *Oxid. Met.* 2002; 58:23.
27. Ul-Hamid A. *Oxid. Met.* 2002; 58:41.
28. Gülgün MA, Voytovych R, Maclaren I, Rühle M, Cannon RM, *Interf. Sci.* 2002; 10:99.
29. Kim JP, Juang HG, Kim KY. *Surf. Coat. Technol.* 1999; 112:91.
30. Türker M. *Corr. Sci.* 1999; 41:1921.
31. Zhou YH, Lin J, Wang SB, Zhang HJ. *Optical Mat.* 2002; 20:13.
32. García-Oca C, Muñoz-Morris MA, Morris DG. *Intermetallics* 2003; 11:425.

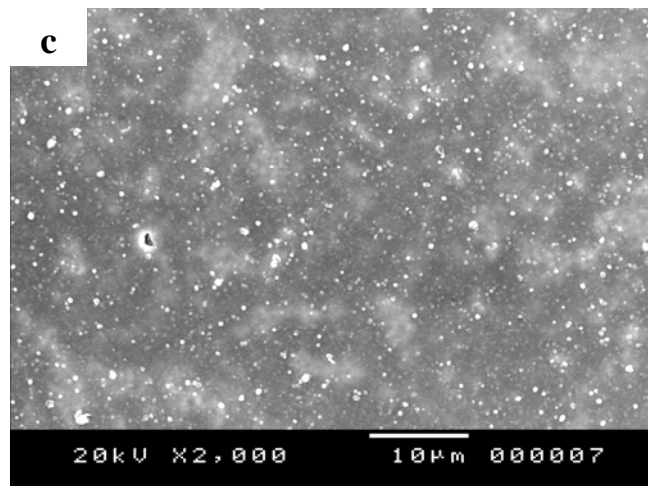
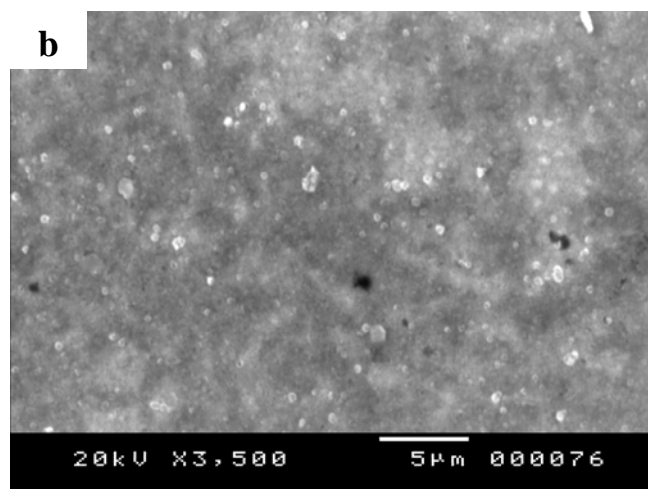
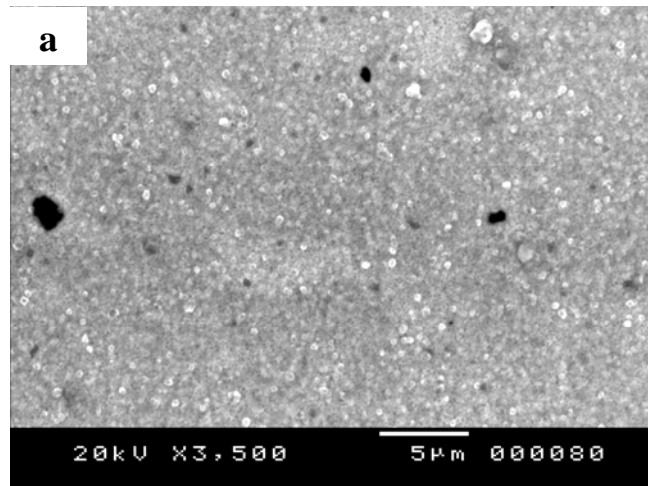


Figure 1.- Densification of the oxide scales after oxidation for 24 h with increasing temperature (a) 850, (b) 900 and (c) 950° C.

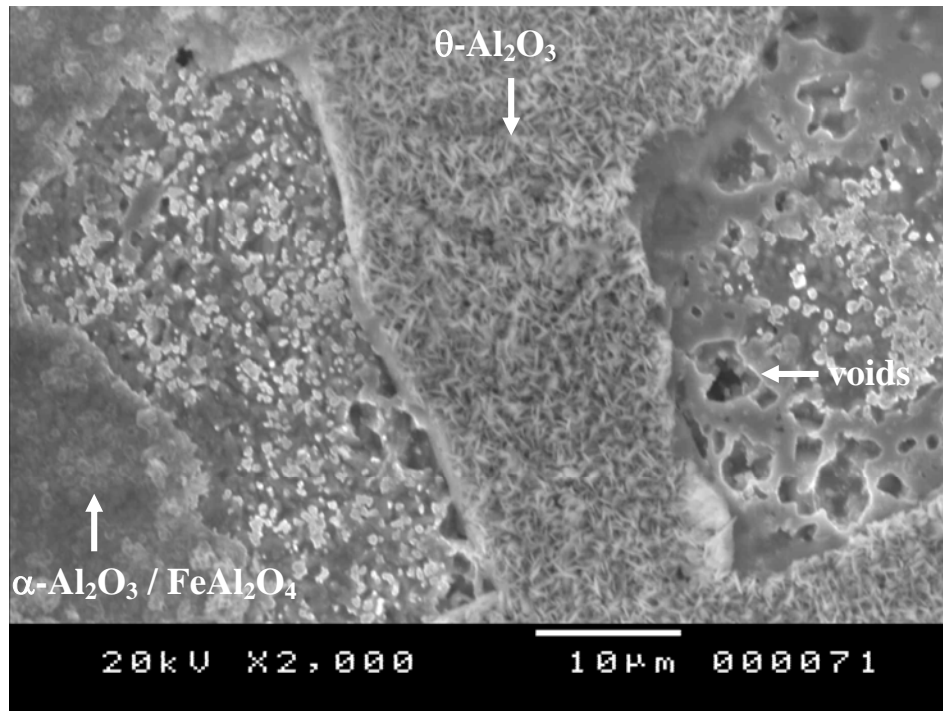


Figure 2.- SEM detail of a spalled zone of the oxide scale developed on FeAl Grade 3 after oxidation at 900° C for 24 h under synthetic air showing different oxide features and voids.

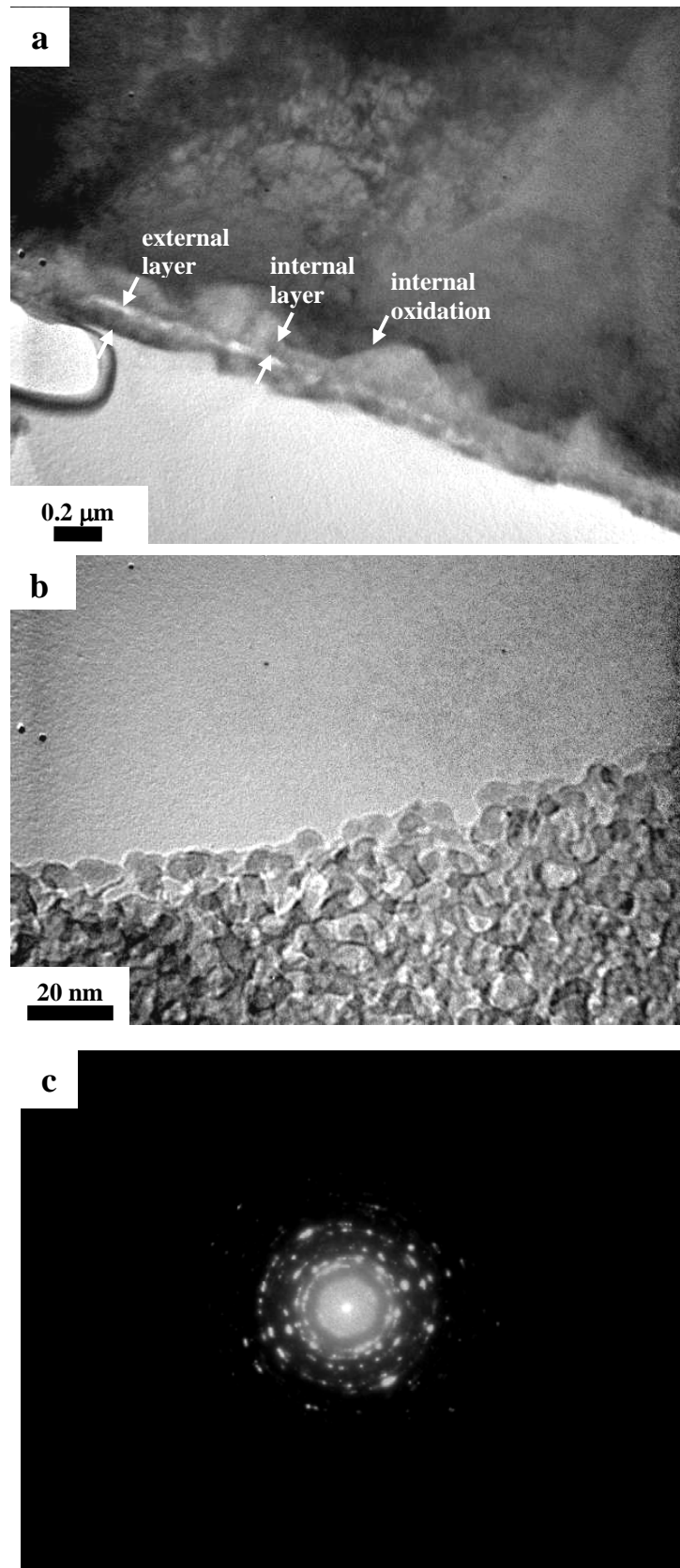


Figure 3.- TEM cross-section of the specimens oxidised at 850° C for 24 h. (a) General view showing the scale divided into two main layers and internal oxidation of the substrate (b) Detail of the top equiaxed morphology at the gas/scale (c) SADP of the overall scale.

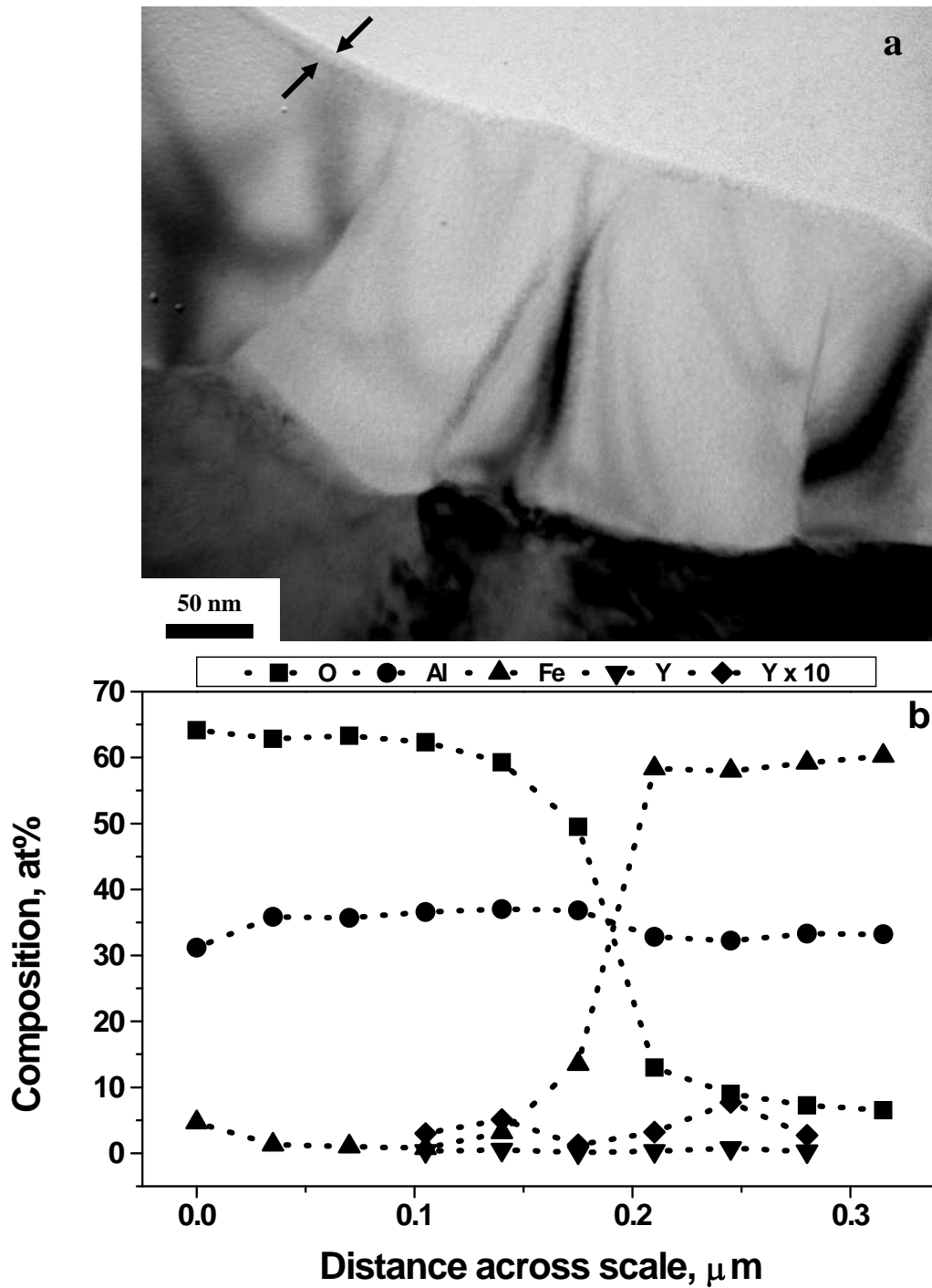


Figure 4.- TEM cross-section of the specimens oxidised at 1000° C for 24 h under synthetic air. (a) General view showing the columnar morphology of the $\alpha\text{-Al}_2\text{O}_3$ grains topped up with equiaxed grains (indicated by arrow marks) and (b) EDS profile (3 nm spot diameter) across the scale.

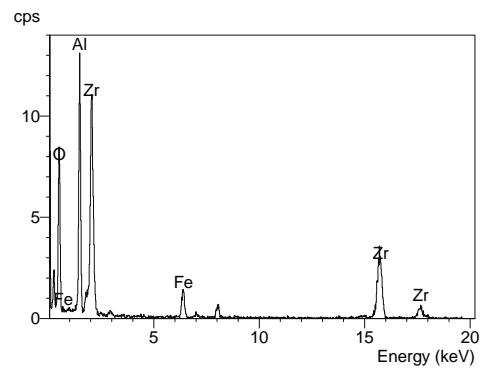
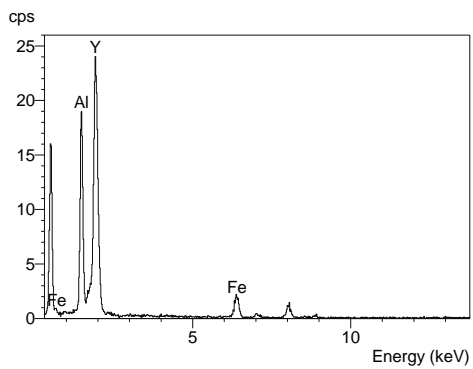
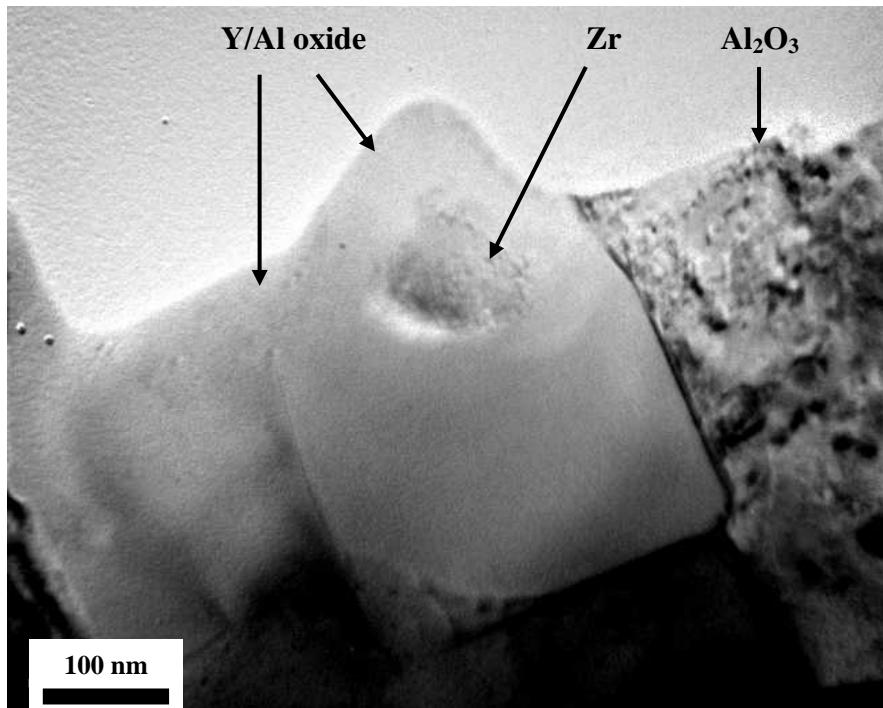


Figure 5.- Y/Al oxide grains irrupting into the alumina scale and Zr segregated within it and their corresponding EDS spectra.